Brazilian Journal of Geophysics (2021) 39(3): 393-411

ISSN 0102-261X
DOI: 10.22564/rbgf.v39i3.2107

CONTRIBUTION OF HYDROGEOPHYSICAL DATA FOR THE ASSESSMENT OF UNCONFINED AQUIFER PROTECTION LEVELS - AN EXAMPLE FROM THE NORTHEAST OF BRAZIL

Alexandre Richardson O. Monteiro and Leandson Roberto F. de Lucena *

ABSTRACT. The use of chemical fertilizers in arable perimeters increases productivity, although it can degrade groundwater quality, particularly if such sources are unconfined. In this context, this paper presents the results of an analysis of the natural protection level of the Barreiras Aquifer in an area located on the eastern coast of northeastern Brazil. Such an aquifer presents an unconfined hydraulic character, making it susceptible to contamination from surface ground loads with contaminants associated with the leaching of excess fertilizers not absorbed by the ground vegetation. The methodology applied is based on the use of hydrogeophysical data, particularly the inverse models of vertical electrical soundings (VESs) and information from well profiles, allowing the acquisition of longitudinal conductance cartographies (S), in mili-Siemens (mS), and aquifer vulnerability using the GOD methodology. Such cartographies are prepared to emphasize the unsaturated overlying zone, highlighting its thickness and occurrence of clay lithologies. Thus, the longitudinal conductance cartography and aquifer vulnerability reveal areas more susceptible to contamination in the northeastern and eastern-central sections of the study area, with values ≤10 mS and ≥0.50 mS, respectively.

Keywords: hydrogeophysics, longitudinal conductance, vulnerability, Barreiras Aquifer-Rio Grande do Norte State, Brazil.

RESUMO. A utilização de fertilização química em perímetros agricultáveis proporciona um incremento da produtividade, embora possa ocasionar uma depreciação qualitativa do aquífero, sobretudo se esse for de natureza não confinada. Nesse contexto, o presente trabalho apresenta resultados referentes a uma análise do grau de proteção natural do Aquífero Barreiras em uma área situada no litoral leste do Estado do Rio Grande do Norte-Brasil. O referido aquífero possui caráter hidráulico não confinado, fato esse que naturalmente lhe confere uma maior susceptibilidade à contaminação. Estes contaminantes estariam associados com a lixiviação de excedentes da fertilização não assimilados pela vegetação. A metodologia utilizada foi fundamentada na utilização conjunta de dados hidrogeofísicos, particularmente de modelos inversos de sondagens elétricas verticais-SEVs, e informações de perfis de poços, possibilitando a obtenção de cartografias de condutância longitudinal (S), dada em mili-Siemens (mS), e vulnerabilidade do aquífero com o método GOD. Essas cartografias foram elaboradas com ênfase para a zona não saturada sobrejacente, ressaltando sobretudo sua espessura e ocorrência de litologias argilosas. Dessa forma, o mapa de condutância longitudinal e a vulnerabilidade revelaram áreas mais susceptíveis à contaminação nos setores nordeste e centro-leste da área de estudo, com valores iguais ou inferiores a 10 mS e maiores ou iguais a 0,50 mS, respectivamente.

Palavras-chave: hidrogeofísica, condutância longitudinal, vulnerabilidade, Aquífero Barreiras-RN/Brasil.

*Corresponding author: Leandson Roberto Fernandes de Lucena

Universidade Federal do Rio Grande do Norte - UFRN, Postgraduate degree in Geodynamics and Geophysics - PPGG, Campus Universitário, Lagoa Nova, 59078-970 Natal, RN, Brazil. Phone: +55(84)3342-2237 – E-mails: alexandrerichardson21@gmail.com, leandson.lucena@ufrn.br

INTRODUCTION AND OBJECTIVES

In the literature, there are reports on the influence of agrochemical usage concerning the qualitative degradation of groundwater sources, particularly with fertilizers (Custódio and Llamas, 1983; Fetter, 1993). Agricultural perimeters frequently require large amounts of water for irrigation as well as substantial quantities of chemical fertilization, including nitrogen compounds. The chemical surpluses from these compounds in their oxidized form (nitrate) can eventually reach aquiferous zones, particularly the free surface of water in unconfined aquifers, if they are not assimilated by the vegetation coverage. Thus, the fertilization and irrigation system plays an important role in agricultural productivity, enabling economic development in a specific region, although it is intensive and random, possibly causing environmental problems related to the groundwater quality. Fertilization is important for productivity, but there is an increased risk of groundwater source contamination (Lucena et al., 2013a).

Based on the assumption of a hydrostratigraphy of unconfined aquifers, it can be evaluated that the context involving irrigated agriculture is a threat to groundwater, which features three environmental situations (Fig. 1), considering the same amount of water for irrigation and chemical fertilizer, according to different soil characteristics overlaying the aquifer:

1. Vadose zone relatively thin without clay compounds that may slow contaminant percolation, providing a low protection level;
2. Vadose zone with predominantly sandy composition, similar to the previous one, but thicker, providing a higher protection level than that reported in "A";
3. Vadose zone with clay compounds interspersed, which can slow the progression of leachate contaminants.

For this type of analysis, the contaminant load is modeled as a vertical displacement in the vadose zone. When inserted in the aquifer, it is subjected to the movement of groundwater. In this case, chemical surpluses from additional fertilization that are not assimilated by vegetation are referred to as leachate contaminants.

In an interdisciplinary context, the term vulnerability of aquifers can be defined as the ease with which an aquifer system can be polluted, i.e., its susceptibility to being adversely affected by the contaminant load (Foster and Hirata, 1993; Oni et al., 2017). Furthermore, these authors claimed that this ease is due to the hydraulic inaccessibility of penetrated contaminants and attenuation capacity of the strata above the saturated zone for physical retention and chemical reactions with the contaminant. This interaction will determine the residence time in the unsaturated zone and the delay in the arrival of the contaminant in the aquifer, as well as the degree of attenuation, retention, or disposal, before it reaches the saturated zone (Foster and Hirata, 1993; Foster et al., 2002).

Thus, unconfined aquifers are more susceptible to contamination than confined aquifers, which by definition have an impermeable or semi-impermeable layer at their upper limit. Conversely, unconfined aquifers are naturally more vulnerable to contamination when they do not have a thick layer of coverage (Foster and Hirata, 1993; Foster et al., 2002).

In this context, geophysical methods have been contributing to the sustainable environmental planning of groundwater, primarily via geoelectrical surveys. For example, there is the electrical conductivity cartography, which is directly correlated with soil clay content, the primary component for the retention and deceleration of contaminants toward groundwater levels, thereby favoring biodegradation processes (Kirsch, 2009).

However, according to Kirsch (2009), the hydrogeological source protection is primarily associated with the presence of overlying protective layers with sufficient thicknesses with reduced hydraulic conductivity. These conditions would cause a delay in the vertical

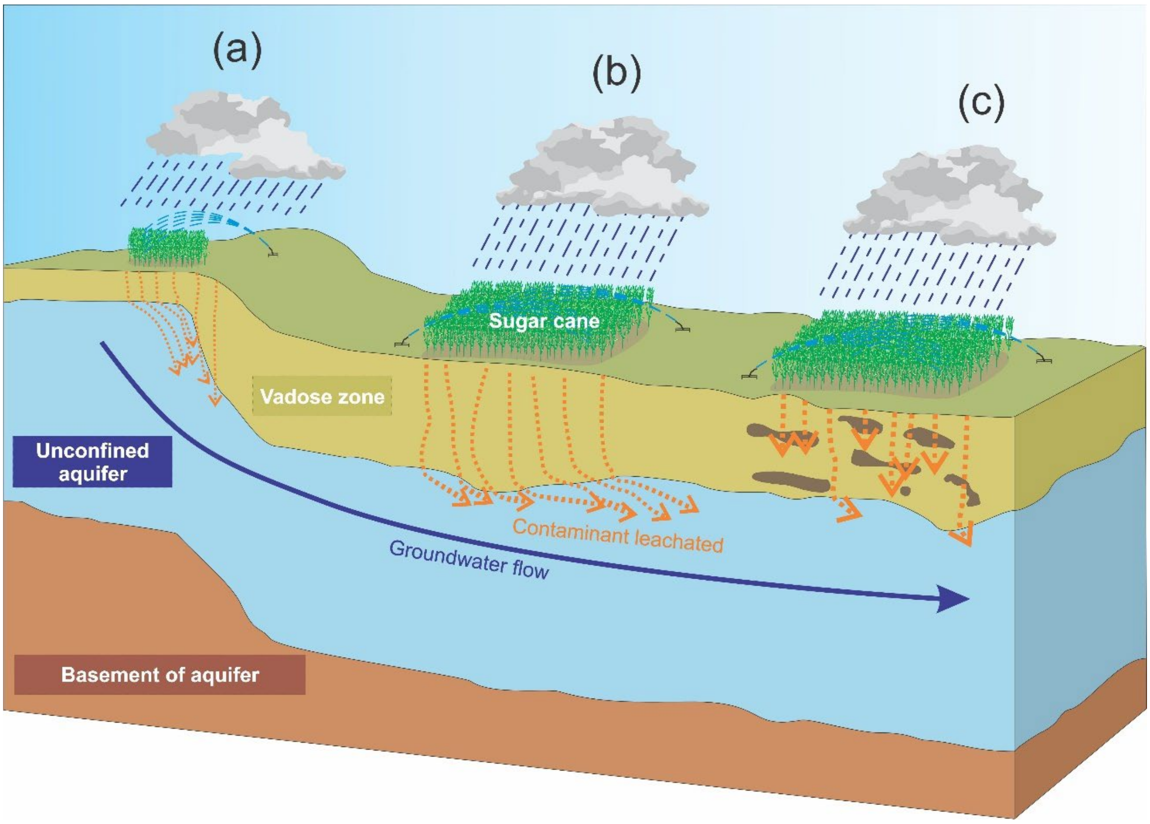

Figure 1 - Different scenarios involving contamination of shallow aquifers in arable perimeters: a) Thin unsaturated zone; b) Thick unsaturated zone; c) Unsaturated zone with lithological clay percentage; the occurrence of clay content and a larger thickness of the unsaturated zone increase the intrinsic physical protection of the aquifer.

movement of the infiltrated solutions, as well as increased degradation of any contaminant mass via bio-physical-chemical reactions (Fetter, 1993; Feitosa et al., 2008). Thus, the geoelectrical parameter of longitudinal conductance from geoelectrical models resistivity vs. thickness enables indirect measurement of thickness and presence of clay layers overlying the aquifer.

In the theory of stratified conductors, the longitudinal conductance is defined as the ratios of thickness and resistivity of the environment under consideration, and it is widely used in the evaluation of groundwater protection capacity (Henriet, 1976; Kalinski et al., 1993; Braga et al., 2006; Braga and Francisco, 2014; Bello et al., 2019; Emberga et al., 2019). In the meantime, the hydraulic conductivity and/or clay content of sediments can be assessed using electrical resistivity, assuming that the lowest resistivities are associated with the highest percentages of clay minerals and/or lower hydraulic conductivity, which interferes with the percolating time of the penetrating solutions in the environment (Henriet, 1976; Kalinski et al., 1993; Braga and Francisco, 2014).

The study area is located on the eastern coast of the State of Rio Grande do Norte in Northeastern Brazil, with the Catu River basin as its geographic boundary, covering approximately 200 km^2 and occupying parts of the municipalities of Canguaretama, Goianinha, Tibau do Sul, and Vila Flor (Fig. 2). The area mentioned is widely used for sugar cane cultivation to produce ethanol and sugar, which is subjected to supplementary NPK-type chemical fertilization (Lucena et al., 2013a).

The primary goal of this research is to quantify the protection level and vulnerability of the Barreiras Aquifer in the mentioned area, which is the primary regional groundwater source with an unconfined hydraulic character. Such quantification will be carried out by

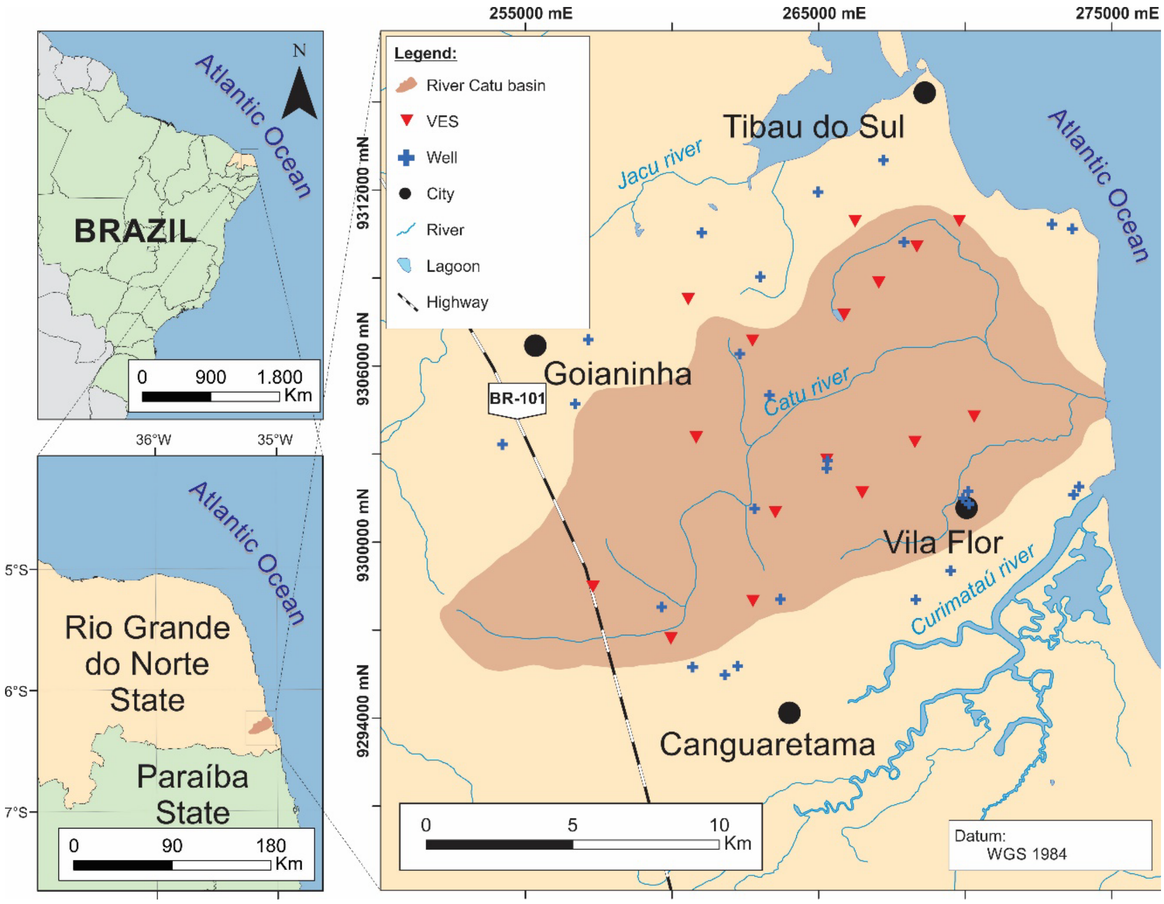

Figure 2 - Location of the Catu River basin-Rio Grande do Norte, Northeastern Brazil.

creating cartographies based on hydrogeophysical data, specific information from the constructive and lithologic profiles of wells, and the use of geoelectrical parameters derived from inverse models of VES.

Geological and hydrogeological settings

The regional stratigraphy consists of two basic sequences: an outcropping and a nonoutcropping. The nonoutcropping sequence consists of a Precambrian crystalline basement and sedimentary rocks of a Mesozoic basin (considering the profile information of regional wells), whereas the outcropping sequence comprises sedimentary Cenozoic rocks of the Barreiras Formation (Tertiary-Quaternary in age) and a Quaternary coverage (Bezerra, 1998; Lucena, 2005; Rossetti et al., 2011; Lucena et al., 2013b; Bezerra et al. 2014; Souza et al., 2019; and Dantas et al., 2021). The crystalline basement is represented by granite, granodiorite, migmatite, and gneisses correlated with the Caicó Complex (Bezerra, 1998; Lucena, 2005). The Mesozoic sediments consist of a sandstone unit (baseline) and other carbonates (top), the latter with sandstone intercalations (Lucena, 2005). This sequence has been correlated with the deposits of the Beberibe (base) and Gramame-Maria Farinha (top) formations, which contain several sandstones and carbonate rocks that are stratigraphically inserted in the coastal sedimentary Pernambuco-Paraíba basin (Bezerra et al., 2001; Rossetti et al., 2011).

The Barreiras formation is an outcropping sequence of siliciclastic Cenozoic lithologies ranging from argillite to conglomerates, with clay sandstones predominating, which are found discordantly overlapping Precambrian rocks of the crystalline basement of the Mesozoic sediments (Lucena, 2005; Souza et al., 2019; Nunes et al., 2019). We have all Quaternary sedimentation heaving the Barreiras formation, distinguishing between subrecent sedimentation (beachrocks and fixed dunes) and recent sedimentation (sandy coverage, silts, moving dunes, besides the sediments of current beaches, and mangroves). This empirical terminology distinguishes between Quaternary lithostratigraphic units that are subject and the ones that are not subject to the current sedimentation processes (Lucena, 2005). Figure 3 depicts the geological outline of the study area (adapted from Dantas et al., 2021).

The Barreiras Aquifer, the stratigraphical unit homonym, has as its low limit in the study area the top of the nonoutcropping carbonatic Mesozoic sequence, which was identified by drilling as being formed by sandy clay and clay sediments of calciferous composition and low hydrogeological potentiality (Lucena, 2005; Silva et al., 2014; Stein et al., 2019; Alves and Lucena, 2021). In terms of hydraulic condition, such source is predominantly unconfined as it is evident by the broad interaction with the surface drainage (the aquifer has natural discharges toward the drainages, besides regional flow toward the coastline), as well as by the results of the aquifer tests performed. The latter revealed values of the order of 2.6×10^{-3} to 3.3×10^{-3} m^2/s of hydraulic transmissivity (T) and 5.98×10^{-5} to 7.58×10^{-3} m/s of hydraulic conductivity (K), considering an average saturated thickness of 40 m (Silva et al., 2014; Souza et al., 2019; Alves and Lucena, 2021). The overlying unsaturated zone, associated with some of the reported Quaternary coverage, comprises sediments or sedimentary rocks of sandy and sandy clay composition.

The Barreiras Aquifer waters in the area are predominantly sodic chlorinated. A universe of 40 analyzed samples has ammonium nitrogen ranging from 0.01 to 2.86 mg/L (11 samples), nitrite contents ranging from 0.03 to 0.63 mg/L (3 samples), and nitrate contents ranging from 0.05 to 6.67 mg/L (37 samples) (Lucena et al. 2013a).

METHODOLOGY

The methodology used in this study was based on the utilization of electric geophysical methods to analyze the protection level of the Barreiras Aquifer in the area of the Catu River hydrographic basin, considering mainly inverse models of vertical electrical sounding (VES), and values of longitudinal conductance (Orellana, 1972; Bello et al., 2019; Kwami et al., 2019; Yusuf et al., 2021). Furthermore, such data were confronted and evaluated as a whole using the Groundwater confinement × Overall lithology × Depth to groundwater table – GOD methodology (Foster and Hirata, 1993; Foster et al., 2002) for the analysis of the local aquifer vulnerability. Those methodological procedures also used information from available well profiles, which partially or totally intercepted the Barreiras Aquifer. Geoelectrical surveying, in particular, was mostly carried out in areas with limited or no information about wells.

Geoelectrical methods are based on determining the electric resistivity of materials that along with dielectric constant and magnetic permeability expresses the electromagnetic properties of soil and rocks (Orellana, 1972; Koefoed, 1979). The electric resistivity of those materials, which has Ohm's Law as its theoretical foundation, indirectly provides the characteristics of the medium (alteration level, fractures, saturation, lithotypes, among other aspects). The current density (J), at any point of a homogeneous isotropic conductor, is proportional to the derivative from the potential related to the distance (dV/dL), and the proportionality factor is represented by the electric conductivity (σ), as shown in Equation 1:

$$J = -\sigma \frac{dV}{dL} \qquad (1)$$

The resistivity of a specific material is the difficulty it imposes on the passage of an electric current, which is the inverse of conductivity. Since the resistivity (ρ) is given in

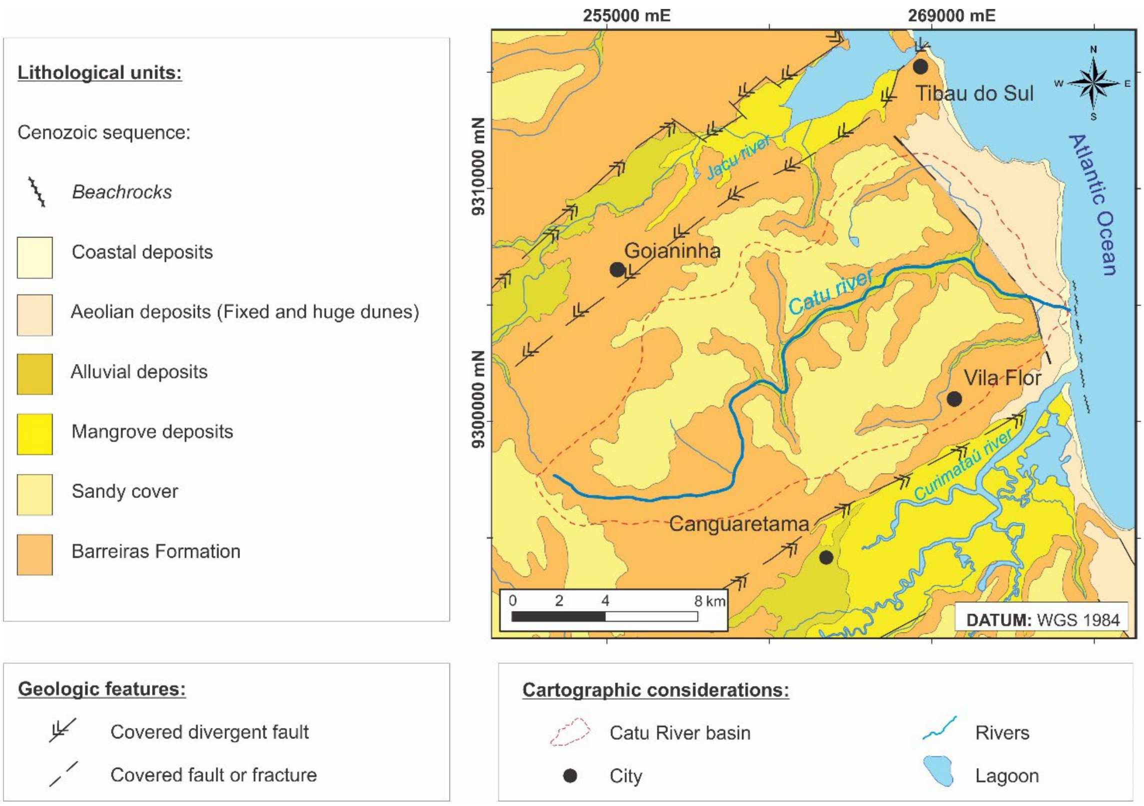

Figure 3 - Geological outline of the area of the Catu River basin-Rio Grande do Norte and vicinity (adapted from Dantas et al., 2021).

ohm m (or Ω·m), the conductivity (σ) is given in Siemens/m (or S/m), as these two parameters are inversely related.

In practical terms, the geophysical methodology of the electroresistivity is considered the difference of measured potential between two points while the measurement of electric current demands the closing of the circuit, and systems in quadrupoles are adopted as a practical device for measuring resistivity (Orellana, 1972).

The geoelectrical technique was used in VES, which consists of injecting electric current into the medium through the current electrodes (A and B) and measuring the potential difference between the potential electrodes (M and N). Thus, the electric current (I) is passed through the subsoil via two electrodes (AB), resulting in a potential difference (ΔV), which is measured by the second pair of electrodes (MN). The value measured for the potential difference is a function of the apparent resistivity of the subsoil and the geometric arrangement of the electrodes (K), where the investigated depths are directly proportional to the spacing between the electrodes (Orellana, 1972). In the Schlumberger array, the potential electrodes are positioned among the current electrodes so that the MN spacing is no more than one-fifth of the AB spacing. In general, the resistivity value (ρ) of the medium can be calculated using the following equations (Orellana, 1972; Koefoed, 1979; Reynolds, 2011):

$$\rho = K\,\frac{\Delta V}{I} \tag{2}$$

$$\rho_a = k_{Schl}\frac{\Delta V}{I} \tag{3}$$

$$k_{Schl} = \frac{\pi\left(\frac{\overline{AB}}{2}\right)^2}{\overline{MN}}\left[1 - \frac{\overline{MN}^2}{4\left(\frac{\overline{AB}}{2}\right)^2}\right] \tag{4}$$

Where:

ρ_a = apparent resistivity;

ΔV = potential difference;

I = electric current;

K_{Schl} = Geometrical factor for the Schlumberger arrangement of electrodes;

$\overline{AB}$ = distance between electrodes A and B;

$\overline{MN}$ = distance between electrodes M and N.

The adopted geoelectrical model, compatible with the geological reality of the area, has the following characteristics:

I. The underground is formed by a sequence of layers with a finite thickness (E_i), except for the last one, which is considered infinite;
II. Each layer is considered electrically homogeneous and isotropic, characterized by a resistivity (ρ_i); and
III. The interfaces between the layers are plane, horizontal, and parallel to the surface of the terrain.

Sixteen geoelectrical sounding data were acquired in the study area and its adjacencies, obtaining resistivity curves in the bi-logarithm graph of "ρ_a × AB/2" for each central point of VES, allowing the subsequent definition of local inverse interpretative models of resistivity vs. thickness. Data on geoelectrical calibrations obtained by Lucena (2005) were used for the quantitative analyses of geoelectrical stratigraphy in the subsurface. Such calibrations were performed on VES contiguous to a well with a known lithologic profile. The calibrated model was obtained in setting the thickness values, based on the information presented in the description of the hydrostratigraphic profile of the well. Thus the best adjustment possible of an interpreted curve (inverse model) to the filed data aims to obtain representative values of substrate resistivity in the subsurface. The maximum aperture of the current electrodes (AB) was 1,200 m, using the Schlumberger electrode array (Orellana 1972; Kirsch 2009). The equipment used for data acquisition was a terrameter resistimeter SAS 300C (ABEM Instrument) (Fig. 4). The IPI2Win software was used to generate the reported inverse models (Bobachev et al., 2000).

The geoelectrical models were equally applied for calculating longitudinal conductance (Maillet, in Orellana, 1972) due to their applicability to hydrogeological studies (Henriet, 1976; Kirsch, 2009; and Braga and Francisco, 2014). The geoelectrical parameter is based on a current flow parallel to the stratifications. A straight prism gives the resistance of the considered layer with square transversal section and sides of unit length as shown below:

$$R_i = \frac{\rho_i L}{S} = \frac{\rho_i}{E_i \cdot 1} = \frac{\rho_i}{E_i} \quad (5)$$

Where:
R_i= resistance of the considered layer (i);
ρ_i = resistivity;
L = length;
E_i = thickness.

Using the inverse parameter of the resistance (conductance-S), as it has an additive property, the conductance Si will be given by:

$$S_i = \frac{E_i}{\rho_i} \quad (6)$$

For the set of the first n layers of the section, we have:

$$S_i = \sum_i \frac{E_i}{\rho_i} \quad (7)$$

The longitudinal conductance highlights a relationship of thickness and resistivity of the layers in the subsurface. Given the possibility of contaminating loads in vertical flow, high relative values of S for overlaying horizons will have a more protected saturated area in the case of aquifer zones. This observation is made because, in the case of clay sedimentary rocks, we would have a high thickness of the overlaying layer or a decrease in the value of the electrical resistivity of that same layer (rocks of smaller hydraulic conductivity). Since the Barreiras Aquifer has a predominantly unconfined local hydraulic nature, as reported (Souza et al., 2019; Alves and Lucena, 2021), this context was applied to the unsaturated zone in the present study.

The GOD methodology was used to analyze the aquifer vulnerability (Foster and Hirata, 1993; Foster et al., 2002). This methodology enables the analysis of an aquifer susceptibility to contamination due to the interaction of the following parameters:

Figure 4 - Aspects of field data acquisition, with Schlumberger electrode array (A) and the used Terrameter SAS 300C resistivimeter (B).

I. ***G****roundwater hydraulic confinement*: hydraulic confinement level, i.e., the condition of the aquifer;

II. ***O****verlaying strata*: lithological substrata occurrence; and

III. ***D****epth to groundwater table*: groundwater table depth, i.e., it corresponds to the unsaturated thickness of overlying aquifers.

The estimate of the vulnerability index involves the following three stages:

1. Identification of the hydraulic confinement level of the Barreiras Aquifer in the area and attribution of a value ranging from 0.0 to 1.0;
2. Knowledge of the lithological characteristics, which will be provided, in this case, by well data and/or geoelectrical soundings, emphasizing that the attributed weight (ranging from 0.4 to 1.0) was considered due to the thickness of the respective occurring lithology;
3. Identification of the water level depth and attribution of a value ranging from 0.6 to 1.0.

In that context, the vulnerability index is obtained by multiplying the values attributed to each parameter ($G \times O \times D$). The result can range from 0 to 1, indicating the classes of natural vulnerability as neglectable, low, average, high, or extreme (Fig. 5). The GOD methodology is used in several studies, with satisfactory results, mainly due to the ease of obtaining and interacting the three parameters involved (Mendonza and Barmen, 2006; Debernardi et al., 2008; Martinez-Bastida et al., 2010; Fernandes et al., 2014). In this study, such punctual vulnerability indices were obtained from well data and inverse geoelectrical models.

The cartographies for the analysis of the protection level, based on the parameter of longitudinal conductance, and the Barreiras Aquifer vulnerability in the study area were obtained from the geoelectrical models of VES and of local vulnerability indices by interpolation and plotting of grids of those data using the SURFER software (2002). The Kriging methodology used interpolation and gridding, employing a spatial dependence among the observations with minimum variance and errors (Christakos, 2000; Loureiro and Lisboa, 2011).

RESULTS AND DISCUSSION

Through the respective inverse models of resistivity vs. thickness, the VES interpretations, allied to geoelectrical calibrations, allowed obtaining information about the local hydrostratigraphy, emphasizing the lithological aspects, and thickness of the unsaturated zone-UZ. Figure 6 shows geoelectric calibration data in the context of the Barreiras Aquifer, adapted from Lucena (2005).

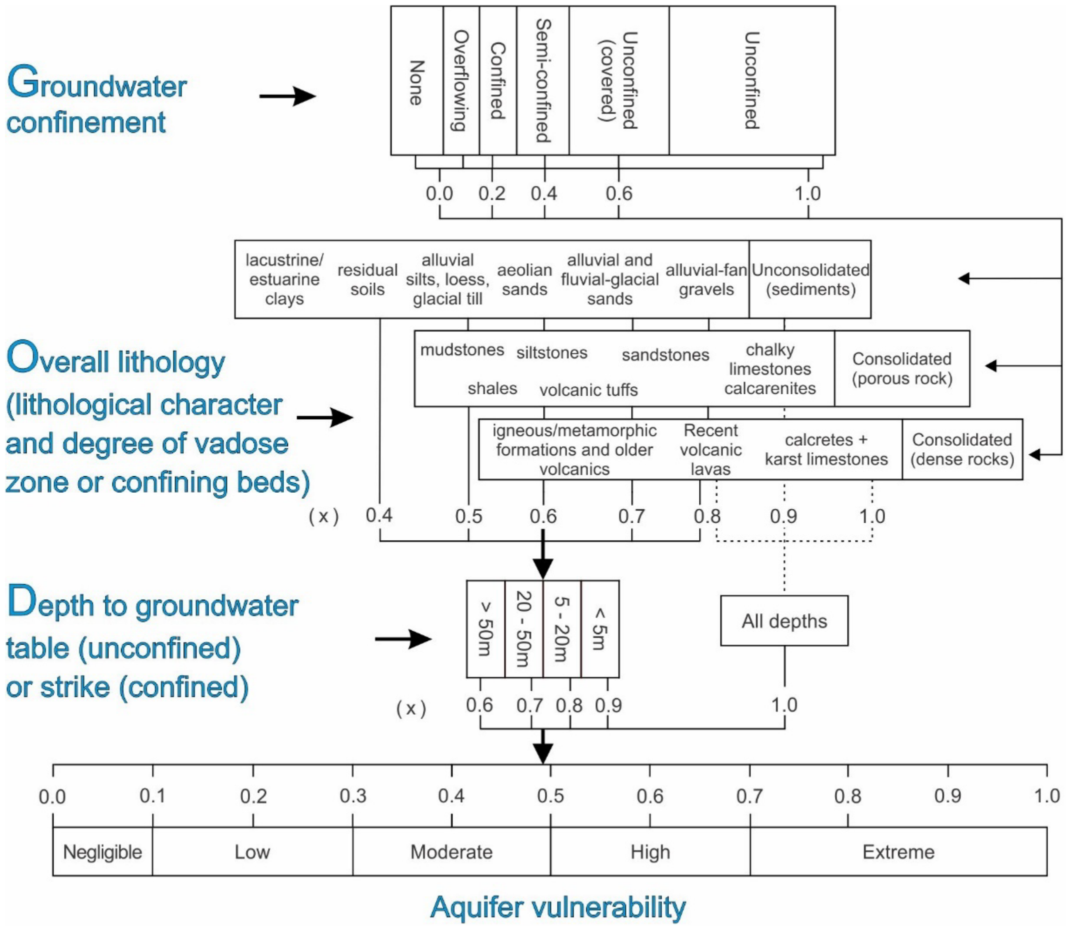

Figure 5 - Flowchart to obtain natural vulnerability indices of aquifers, according to the GOD methodology (Foster and Hirata, 1993; Foster et al., 2002).

Table 1 presents the values of unsaturated thickness from the VES inverse models.

Table 1 - UTM (m) coordinates of VES and their respective thickness values of the unsaturated zone.

VES	UTM X (m)	UTM Y (m)	Unsaturated zone (m)
1	259948	9296646	19.6
2	257278	9298415	66.0
3	262757	9297930	32.0
4	260539	9308256	12.0
5	266251	9310920	17.0
6	269823	9310928	25.5
7	268370	9310058	4.7
8	270330	9304236	25.0
9	268304	9303375	6.5
10	266500	9301640	11.2
11	263523	9300966	24.6
12	260812	9303524	7.0
13	262745	9306840	20.0
14	265875	9307718	34.0
15	267062	9308822	3.0
16	265282	9302766	19.5

In terms of qualitative analysis, VES was consistent with the local hydrogeological context, as indicated by the well profiles, particularly in the association of geoelectrical layers with lithological layers. Resistivity variations were observed in the most superficial levels, between 140 and 10.500 Ωm, associated with the lithology variation, predominantly the clayey and sandy ones, respectively, as well as geoelectric responses congruent with the saturation zone with resistivities from 500 to 900 Ωm for the sandiest layers. The electrode openings used allowed for an investigation depth, covering up to the hydrogeological base of the Barreiras Aquifer, represented by the top of the regional carbonate sequence, with a conductive geoelectric nature (resistivities in the order of 50 Ωm).

Table 2 depicts the reported inverse models of VES (geoelectrical stratigraphy), particularly for the UZ and the respective calculation of the longitudinal conductance,

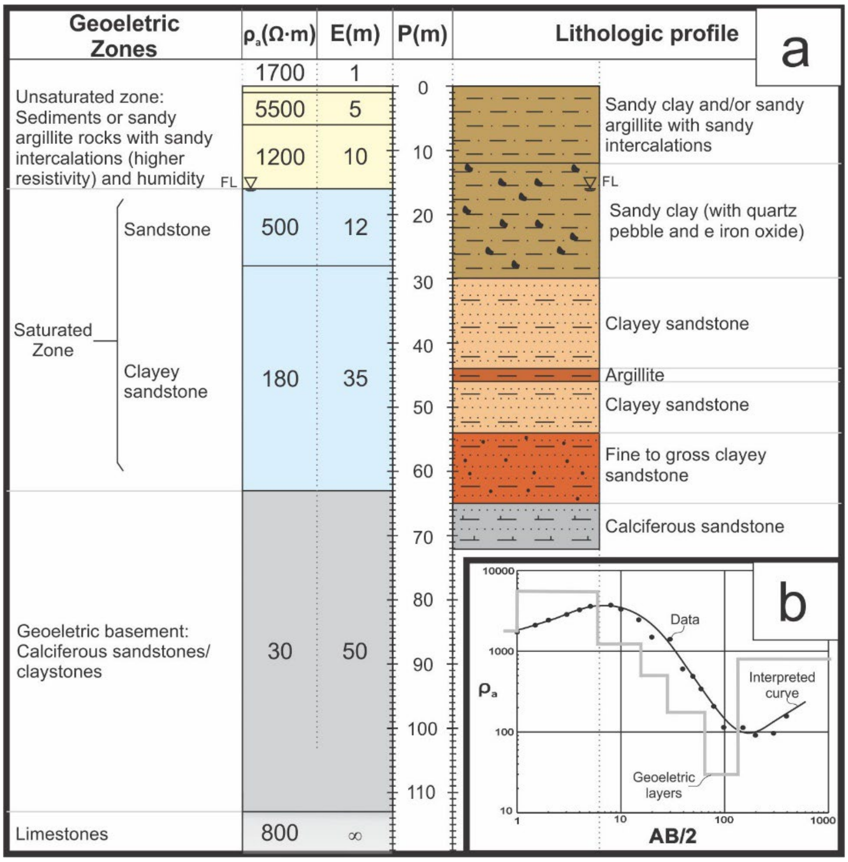

Figure 6 - Geoelectric hydrostratigraphy of calibration (A); the graph represents the adjustment of the modeled curve to the field data (B); the phreatic level (FL) is at a depth of 16.0 (adapted from Lucena, 2005); the geoelectrical calibration between resistivity and lithologies is used in the interpretation of the other VESs.

elaborated according to Equation 7. The data from the longitudinal conductance calculation, shown in Table 2, were submitted to interpolation and gridding to produce longitudinal conductance cartographies. Even though, such parameter is given by the quotient between the resistivity and thickness factors. A medium with reduced values of S is associated with the relatively reduced thickness or high resistivities, particularly in the unsaturated zone. This case is predominantly compatible with sediments or sedimentary rocks in that lithotype has higher infiltration rates, indicating a higher vertical permeability, making the aquifer more susceptible to contaminating loads. We have a more protected aquifer in the subareas where the S parameter is higher, since it has a higher thickness overlaying it. This situation grants higher filtration during the contaminating load percolation, protecting underground waters. Alternatively, the high S value can be related to reduced resistivities of the UZ, a fact, i.e., characteristic of predominantly clayey lithologies with smaller vertical permeability. In this case, a certain contaminating load hinders the hydraulic accessibility to the saturated zone.

Figure 7 depicts a variation map of the values obtained from the S data interpolation and gridding, which rang from 5 mS to 55 mS. Using the isoline of 20 mS as an intermediate reference value, it is found that the Barreiras Aquifer is less protected in the northeastern and eastern-central sections of the map, with longitudinal conductances around 10 mS, to the detriment of values of S greater than 30 mS in the southwestern section, which is associated with a higher level of the source protection.

However, this is an analysis of the protection level of an unconfined aquifer based on geoelectrical survey values; the sensitivity of such methodology is demonstrated by the rainfall occurrence before the field survey. In this aspect, obtaining geoelectrical data (and the subsequent longitudinal conductance

Table 2 - Geoelectrical stratigraphy for the 16 VES and the respective values of longitudinal conductance. h_1 to h_4 and ρ_1 to ρ_4 represent thicknesses and resistivities of the UZ layers, from the most superficial layer to the deepest one, respectively.

VES	Unsaturated thickness (m)				Resistivity (Ohm.m)				S (mS)
	h_1	h_2	h_3	h_4	ρ_1	ρ_2	ρ_3	ρ_4	
1	1.6	18.0	-	-	460	1100	-	-	19.8
2	0.5	8.5	57.0	-	400	3000	1150	-	53.6
3	0.5	0.5	1.0	30.0	450	2200	200	900	39.7
4	2.5	2.5	7.0	-	1350	300	4500	-	11.7
5	2.0	8.0	7.0	-	1000	600	1300	-	20.7
6	0.5	0.5	2.5	22.0	1100	2200	1200	3300	9.4
7	0.7	4.0	-	-	980	3400	-	-	1.9
8	1.0	2.0	12.0	10.0	2000	3300	850	2700	18.9
9	0.5	6.0	-	-	500	1400	-	-	5.3
10	1.2	4.0	6.0	-	2000	1000	2000	-	7.6
11	0.6	12.0	12,0	-	1500	950	4000	-	16.0
12	0.5	0.5	6.0	-	300	2500	450	-	15.2
13	10.0	10.0	-	-	600	2000	-	-	21.7
14	2.0	2.0	30.0	-	450	140	1400	-	40.2
15	0.5	0.5	2.0	-	300	10000	3000	-	2.4
16	1.0	4.0	14.5	-	10500	3000	2000	-	8.7

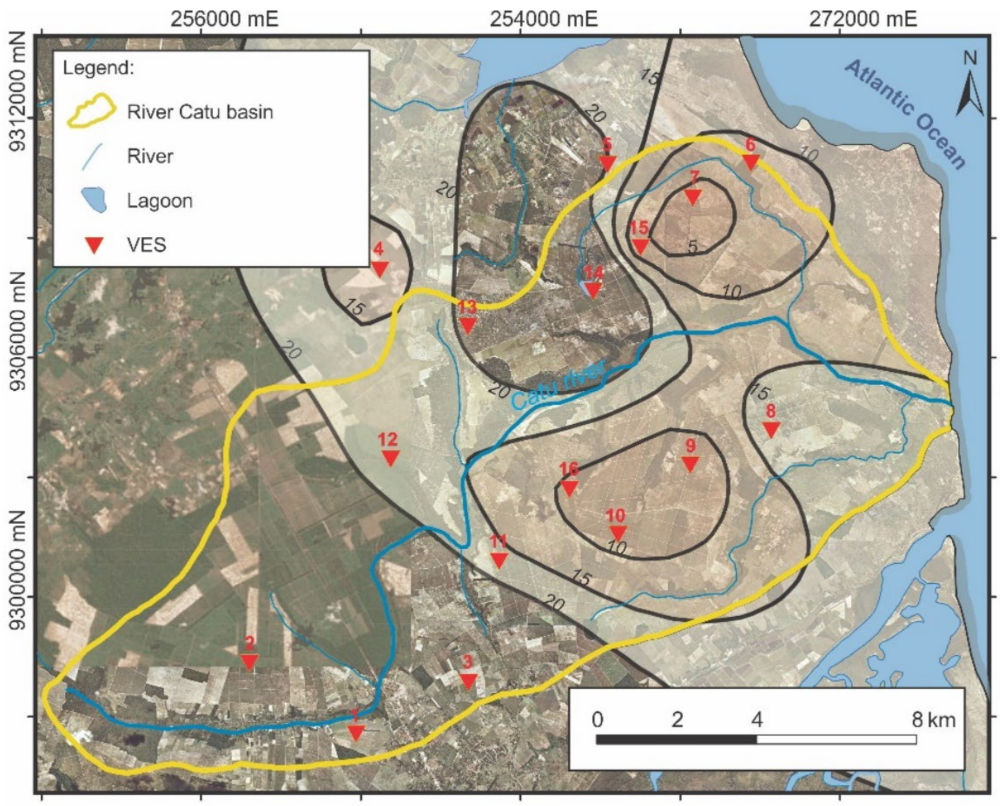

Figure 7 - Longitudinal conductance cartography (S) in the area of the Catu River hydrographic basin (Rio Grande do Norte); the isolines show the values of S in mS (10^{-3} Siemens); values smaller than 10 mS identify locations that are more susceptible to contamination (less intrinsic protection of the aquifer).

determination) on days following rainfall can result in ambiguous geoelectric interpretations, particularly with regard to values of apparent resistivities of the unsaturated zone layers and their respective associated lithologies. Thus, the resistivity reduced values can be associated with additional residual humidity in the unsaturated zone rather than just with the occurrence of layers with more clay, which would provide a greater protection to the aquifer.

The protection level of an unconfined aquifer, considering values from the geoelectrical survey and the sensibility of the methodology, is verified in the rainfall occurrence before the field survey. Thus, obtaining geoelectrical data (and the subsequent longitudinal conductance determination) on days after the rainfall occurrence leads to ambiguous geoelectric interpretations, primarily concerning the values of apparent resistivities of the layers on the unsaturated zone and their respective associated lithologies.

Reduced resistivity values can thus be associated with additional residual humidity in the unsaturated zone, rather than just with the presence of layers with more clay, which would provide greater protection to the aquifer.

Similarly, geoelectric surveys carried out at the end of the annual drought period in the area can induce geoelectric interpretations that result in overestimated values in terms of the UZ thickness. Such observation is supported by high infiltration speeds in the vadose zone determined by Lucena et al. (2013a) in infiltration tests performed in the Catu River basin (Rio Grande do Norte).

We can also propose a graphic classification of the protection level of the Barreiras Aquifer based on the geoelectrical data presented here, correlating the thickness and representative resistivity parameters of the unsaturated zone, in addition to the values of longitudinal conductance (Fig. 8). That ternary graphic configuration for the aquifer protection analysis was initially proposed by Braga (2008), although he considered the presence of overlying aquitard to the analyzed aquifer to the detriment of the context of the unconfined aquifer of this study.

It is emphasized here that to the detriment of resistivity individual values of the different geoelectrical layers of the unsaturated zone, a single representative resistivity was considered, using the pseudo-anisotropy concept described by Orellana (1972). This author proposes that the different layers considered homogeneous and isotropic in the mathematical-geophysical mode may behave as a single anisotropic medium of resistivity ρm.

Therefore, a representative resistivity value of the entire UZ was adopted, corroborating the obtained S values, together with the respective unsaturated thickness (Fig. 8). In the aforementioned graphical analysis, fields of low, intermediate, and high protection levels were delimited, according to the configuration of the longitudinal conductance map (with the adopted intermediate value of 20 mS), besides the geoelectrical calibrations.

Analyzing the reported graph, we see that the thickness parameter of the unsaturated zone predominates in terms of intrinsic physical protection of the source. Conversely, for situations of approximate equivalence of that parameter in different VES, the positioning of them in the graph was determined by the lithological composition (as interpreted in the inverse models based on geoelectrical calibrations). Considering VES-05 and VES-16 as examples, we observed that they are equivalent in the dimensional aspect of the unsaturated thickness. However, their classifications diverge to the detriment of the resistivity values, since the identified UZ in VES-05 is compatible with a composition higher in clay than that determined in VES-16. Taking VES-10 and VES-11 as examples, the preponderance of the thickness values of the UZ occurs in the class classification. Thus, we have an equivalence in the resistivity values; however, their classifications differ due to the first having a thinner UZ.

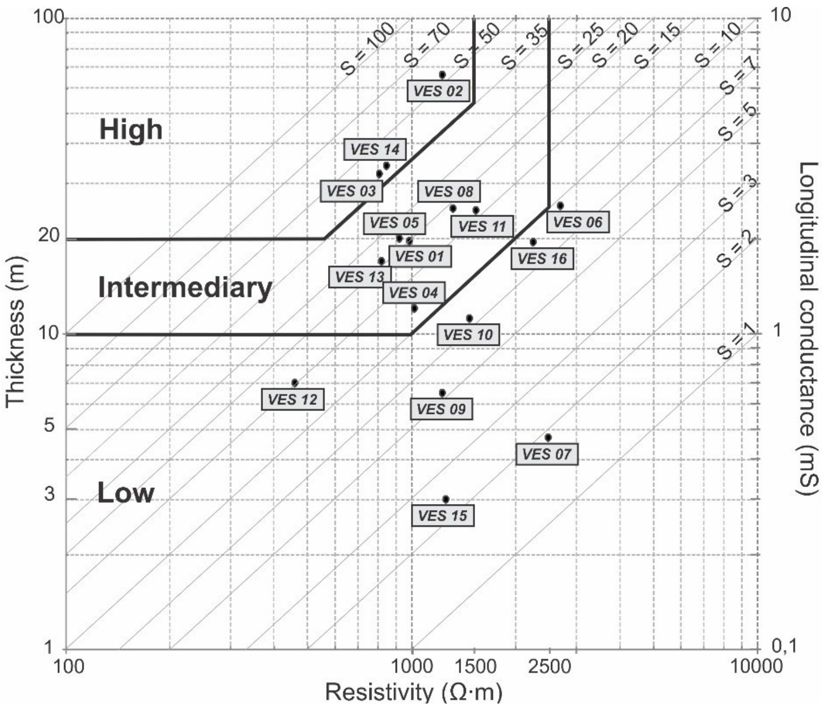

Figure 8 - Relation between "longitudinal conductance x thickness x resistivity" of the UZ and the intrinsic protection level of the Barreiras Aquifer, Catu River hydrographic basin area (RN) (adapted from Braga, 2008).

Although based on the GOD methodology (Foster and Hirata, 1993; Foster et al., 2002), the index determination of the local vulnerability of the Barreiras Aquifer was defined based on hydrogeological and geophysical data, as opposed to only hydrogeological information in the original conceptualization of the method. Consequently, the aforementioned parameters, for determining the vulnerability indices, were obtained from available well profiles and also from the inverse model information of the geoelectrical soundings. The adoption of that multidisciplinary methodology to assess the vulnerability resulted from the fact that in some local subareas the well information was scarce or even inexistent, situations in which the geoelectrical sounding was preferentially performed, as reported.

The parameters evaluated in the GOD index of vulnerability (UZ thickness, UZ lithology, and aquifer type) for well data (Table 3) were obtained directly from the respective profiles.

However, calibration and geoelectrical information was used to analyze those parameters based on geophysical data, emphasizing the unsaturated zone. In this case, the GOD methodology parameter associated with lithological characteristics was established with weighing factors ranging from 0.5 to 0.7, and also depending on whether its content was higher in clay or sand, respectively (Table 4). Table 5 depicts the natural vulnerability indices of the Barreiras Aquifer, which has an unconfined hydraulic character throughout the study area.

Figure 9 shows an integrated synthesis of the natural vulnerability analysis of the Barreiras Aquifer. In the northeastern and southwestern ends, we have the highest and lowest vulnerability indices, respectively, with greater influences on the UZ dimensional aspect.

The cartography confirmed the observations based on the longitudinal conductance map about the GOD vulnerability index. Thus, using 0.45 as an intermediate index, we can see areas that are more susceptible to contamination (GOD index equal to or greater than 0.50) and those with more conditions of natural protection (GOD index smaller than or equal to 0.40). In this context, the general vulnerability of the Barreiras Aquifer in the area is moderate to high using the GOD methodology.

Table 3 - UTM Coordinates (m) of the wells and the respective values of thickness and predominant lithological composition of the unsaturated zone in the Catu River basin area (Rio Grande do Norte).

Well	UTM N (m)	UTM E (m)	Unsaturated thickness (m)	Lithological character
1	9295414	261805	39.5	Sandstone
2	9295700	260700	38.0	Argillite
3	9295730	262228	31.0	Sand, clay, and sandstone
4	9297750	259650	27.0	Sandstone
5	9298000	263700	30.0	Clay and sandstone
6	9298000	268300	2.0	Clayey sand
7	9299000	269500	6.5	Clay
8	9301108	262828	5.0	Sand and argillite
9	9301274	270137	26.5	Sand, clay, and argillite
10	9301458	269926	7.5	Sandy clay
11	9301600	273700	19.0	Argillite
12	9301700	270100	22.0	Sandstone
13	9301874	273886	41.5	Sand, sandstone, and argillite
14	9302466	265282	19.5	Sand and silty clay
15	9302750	265294	17.0	Silt, sandstone, and argillite
16	9303300	254200	27.5	Argillite
17	9304700	256700	32.0	Argillite
18	9305004	263328	28.0	Sandstone
19	9306400	262300	23.0	Silt
20	9306856	257150	3.5	Sandy-clayey soil and clay
21	9309000	263000	33.0	Argillite
22	9310196	267915	29.0	Argillite and sandstone
23	9310500	261000	11.5	Sandstone
24	9310644	273679	29.5	Sand-silty clay
25	9310800	272950	20.0	Sand and sandstone
26	9311900	265000	5.5	Sandstone
27	9313000	267200	24.5	Argillite

Table 4 - Weighing factors associated with the ranges of apparent resistivity and characteristics of the considered lithological medium.

Apparent resistivity (ρ)(Ω·m)	Weighing factor	Characteristics of the lithological medium
ρ < 1000	0.5	Sediments and/or sedimentary rocks of mainly clayey composition;
1000 < ρ < 2500	0.6	Sediments and/or sedimentary rocks of sandy-clayey to sandy composition, respectively associated to smaller and bigger values of resistivity;
ρ > 2500	0.7	Sediments and/or sedimentary rocks of gross sandstone to conglomerate composition.

Table 5 - Weighing factors and GOD indices of local vulnerability attributed to wells and VES; the parameters G, O, and D refer to the occurrence type of the aquifer, lithology type of the UZ, and the water table depth or thickness of the UZ, respectively.

DATA	Parameters			***GOD* index**
	G	***O***	***D***	
Well-01	1	0.7	0.7	0.5
Well-02	1	0.5	0.7	0.4
Well-03	1	0.6	0.7	0.4
Well-04	1	0.7	0.7	0.5
Well-05	1	0.6	0.7	0.4
Well-06	1	0.6	0.9	0.5
Well-07	1	0.5	0.8	0.4
Well-08	1	0.6	0.9	0.5
Well-09	1	0.6	0.7	0.4
Well-10	1	0.6	0.8	0.5
Well-11	1	0.5	0.8	0.4
Well-12	1	0.7	0.7	0.5
Well-13	1	0.6	0.7	0.4
Well-14	1	0.6	0.8	0.4
Well-15	1	0.6	0.8	0.5
Well-16	1	0.5	0.7	0.4
Well-17	1	0.5	0.7	0.4
Well-18	1	0.7	0.7	0.5
Well-19	1	0.5	0.7	0.4
Well-20	1	0.6	0.9	0.5
Well-21	1	0.5	0.7	0.4
Well-22	1	0.6	0.7	0.4
Well-23	1	0.7	0.8	0.6
Well-24	1	0.6	0.7	0.4
Well-25	1	0.7	0.8	0.6
Well-26	1	0.7	0.8	0.6
Well-27	1	0.5	0.7	0.4
VES-01	1	0.6	0.8	0.5
VES-02	1	0.6	0.6	0.4
VES-03	1	0.5	0.7	0.4
VES-04	1	0.6	0.8	0.5
VES-05	1	0.6	0.8	0.4
VES-06	1	0.7	0.7	0.5
VES-07	1	0.7	0.9	0.6
VES-08	1	0.6	0.7	0.4
VES-09	1	0.6	0.8	0.5
VES-10	1	0.6	0.8	0.5
VES-11	1	0.6	0.7	0.4
VES-12	1	0.5	0.8	0.4
VES-13	1	0.6	0.8	0.4
VES-14	1	0.6	0.7	0.4
VES-15	1	0.7	0.9	0.6
VES-16	1	0.6	0.8	0.5

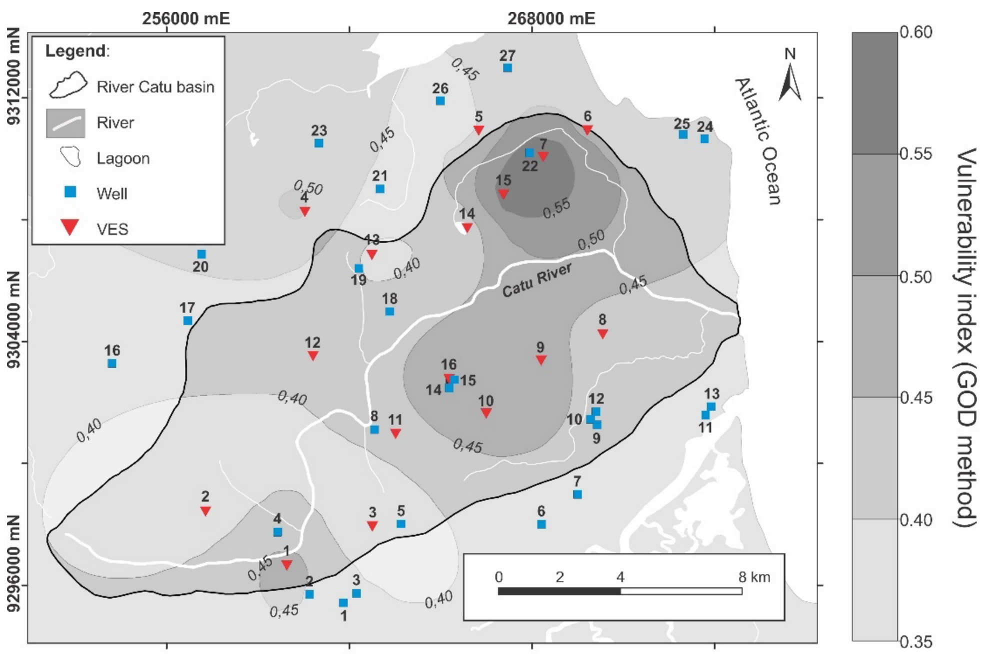

Figure 9 - Map of the vulnerability indices of the Barreiras Aquifer based on the GOD methodology (Foster and Hirata, 1993; Foster et al., 2002), in the area of the Catu River hydrographic basin (Rio Grande do Norte).

Given the noninvasive applicability of the geophysical method used, the obtained results were promising as auxiliary tools for the sustainable hydrogeoenvironmental management of the studied area. In addition to its adoption by governmental agencies managing hydro resources, such methodology can contribute to agribusiness by subsidizing the optimization of the complementary fertilization use. This optimization would result from using more or less quantitative fertilizers, in spite of taking into account their assimilation capacity by the considered vegetable coverage in areas that are naturally more or less protected in terms of their underground waters.

CONCLUSIONS

In conceptual terms, it can be considered that while both terms refer to the degradation possibility of the underground source, the protection level and aquifer vulnerability have connotations derived from classic geophysical and hydrogeological analyses. In this context, the contamination possibility of the Barreiras Aquifer in the study area was considered due to the lixiviation of excessive chemical fertilizers, highlighting the nitrogenized ones used as fertilizer for the cultivated perimeters in the area. This observation is supported by local concentrations of nitrate exceeding 5 ml/L, already denoting a tendency to contaminate the underground waters, and the consequent use of complementary fertilization added to the sugarcane crop in perimeters exceeding 90% of the study area.

Individually, the longitudinal conductance cartography emphasized protection levels that the overlaying physical medium, associated with the unsaturated zone, provides to the underground waters, considering the unconfined local hydraulic nature of the aquifer. Using 20 mS as the intermediate value, 10 mS and 30 mS were used to identify locations that are more and less susceptible to contamination, respectively. In the graphic representation of this geoelectrical parameter, three fields were proposed and delimited in terms of the protection degree of the Barreiras Aquifer: low, intermediate, and high protection levels, considering the respective values of thickness, resistivity, and longitudinal conductance of the unsaturated zone obtained from VES inverse models. Despite the existence of anecdotal cases, in which the lithological composition governs this aquifer condition, the resistivity occurrence, associated with clay content in the unsaturated zone and including the thickness parameter predominance of the unsaturated zone, was observed in terms of intrinsic physical protection of the source.

The analysis of the source protection degree was corroborated by the aquifer vulnerability cartography using the GOD methodology. However, due to a greater number of samples (VES and wells), the GOD methodology has presented better-defined subareas in terms of vulnerability. The vulnerability indices of 0.50 and 0.40, respectively, include areas of the northeastern and southwestern ends of the study area, which are more and less vulnerable to the potential contaminating load imposed on the surface, respectively.

The new methodology based on hydrogeophysical data has proven to be effective, noninvasive, and a low-cost tool, particularly for environmental management. Its applicability in similar hydrogeological terrains can only be feasible by using 1D geoelectric models, in the form of longitudinal conductance cartography, or by composing a vulnerability analysis, supplementing well data when available.

ACKNOWLEDGMENTS

The authors would like to thank the National Council for Scientific and Technological Development-CNPq (Conselho Nacional de Desenvolvimento Científico e Tecnológico - Brazilian Government) for funding this research.

REFERENCES

Alves RS, Lucena LRF. 2021. Uso de dados hidrogeofísicos e modelos numéricos como alternativa na otimização de locações de poços em um aquífero não confinado. Revista Águas Subterrâneas, 35(1): 51-64. Doi: 10.14295/ras.v35i1.29987.

Bello R, Balogun AO, Nwosu UM. 2019. Evaluation of Dar Zarrouk parameters of parts of Federal University of Petroleum Resources, Effurun, Nigeria. J. Appl. Sci. Environ. Manage., 23(9): 1709-1715. Doi: 10.4314/jasem.v23i9.16

Bezerra FHR. 1998. Neotectonics in Northeastern Brazil. Ph.D. Thesis, University of London, 1998. 208 pp.

Bezerra FHR, Amaro VE, Vita-Finzi C, Saadi A. 2001. Pliocene-Quaternary fault control of sedimentation and coastal plain morphology in NE Brazil. Journal of South American Earth Sciences, 14: 61-75. Doi: 10.1016/S0895-9811(01)00009-8

Bezerra FHR, Rossetti DF, Oliveira RG, Medeiros WE, Brito Neves BB, Balsamo F, Nogueira FCC, Dantas EL, Andrades Filho C, Góes AM. 2014. Neotectonic reactivation of shear zones and implications for faulting style and geometry in the continental margin of NE Brazil. Tectonophysics, 614: 78-90. Doi: 10.1016/j.tecto.2013.12.021

Bobachev AA, Modin IN, Shevnin VA. 2000. IPI2Win v. 2.1, IPI_RES2, IPI_RES3, User's Guide. Geoscan-M Ltd., Moscow, 25 pp.

Braga ACO, Malagutti Filho W, Dourado JC. 2006. Resistivity (DC) method applied to aquifer protection studies. Revista Brasileira de Geofísica, 24(4): 573-581. Doi: 10.1590/S0102-261X2006000400010

Braga ACO. 2008. Estimativa da vulnerabilidade natural de aquíferos: uma contribuição a partir da resistividade e condutância longitudinal. Revista Brasileira de Geofísica, 26(1): 61-68. Doi: 10.1590/S0102-261X2008000100005

Braga ACO and Francisco, RF. 2014. Natural vulnerability assessment to contamination of unconfined aquifers by longitudinal conductance – (S) Method. Journal of Geography and Geology, 6(4): 68-79. Doi: 10.5539/jgg.v6n4p68

Christakos G. 2000. Modern Spatiotem poral Geostatistics. New York: Oxford Univ. Press, 288 pp.

Custódio E and Llamas MR. 1983. Hidrología subterrânea. Ed. Omega, Barcelona, Vol. 1 and 2. 2350 pp.

Dantas EP, Medeiros VC, Cavalcante R. 2021. Mapa geológico do Estado do Rio Grande do Norte. Recife: Serviço Geológico do Brasil-CPRM. 1 color map.132,72cm x 85,45cm.

Scale 1:500.000. Programa Geologia, Mineração e Transformação Mineral. Ação: Levantamentos Geológicos e Integração Geológica Regional. Available in cprm.gov.br, accessed on August 20, 2021.

Debernardi L, Luca DA, Lasagna M. 2008. Correlation between nitrate concentration in groundwater and parameters affecting aquifer intrinsic vulnerability. Environmental Geology, 55: 539-558. Doi: 10.1007/s00254-007-1006-1

Emberga TT, Opara AI, Onyekuru SO, Omenikolo IA, Nkpuma OR, Nchedo EM. 2019. Regional Hydro-geophysical Study of the groundwater potentials of the Imo River Basin southeastern Nigeria using superficial resistivity data. Australian Journal of Basic and Applied Sciences, 13(8): 76-94. Doi: 10.22587/ajbas.2019.13.8.12

Feitosa ACF, Manoel Filho J, Feitosa EC, Demetrio JGA. 2008. Hidrogeologia – conceitos e aplicações. 3rd ed., rev. and expanded. Rio de Janeiro, RJ, Brazil: CPRM: LABHID, 812 pp.

Fernandes LFS, Cardoso LVRQ, Pacheco FAL, Leitão S, Moura JP. 2014. DRASTIC and GOD vulnerability maps of the Cabril River Basin, Portugal. Civil Engineering, R. Esc. Minas, Ouro Preto, 67(2): 133-142. Doi: 10.1590/S0370-44672014000200002.

Fetter CW. 1993. Contaminant Hydrogeology. University of Wisconsin-Oshkosh, USA. Prentice Hall, 2nd ed., 497 pp.

Foster SSD and Hirata RCA. 1993. Determinação do risco de contaminação das águas subterrâneas: um método baseado em dados existentes. São Paulo, SP, Brazil: Instituto Geológico, Boletim n. 10: 67-92.

Foster SSD, Hirata RCA, Gomes D, D'Elia M, Paris M. 2002. Groundwater Quality Protection: a guide for water utilities, municipal authorities and environment agencies. Groundwater Management Advisory Team, WHO/PAHO/CEPIS and UNESCO/ROSTLAC/PHI, The World Bank, Washington, D.C. 103 pp.

Henriet JP. 1976. Direct applications of the Dar Zarrouk parameters in ground water surveys. Geophysical Prospecting, 24: 344-353. Doi: 10.1111/j.1365-2478.1976.tb00931.x

Kalinski RJ, Kelly WE, Bogardi, I, Pesti G. 1993. Electrical resistivity measurements to estimate travel times through unsaturated ground water protective layers. Journal of Applied Geophysics, 30: 161-173. Doi: 10.1016/0926-9851(93)90024-S

Kirsch R. 2009. Groundwater Geophysics: A tool for Hydrogeology. Ed. Springer, Germany. 493 pp.

Koefoed O. 1979. Geosounding Principles, 1: Resistivity Sounding Measurements. Elsevier Scientific Publishing Company, Amsterdam, Oxford, New York. 276 pp.

Kwami IA, Ishaku JM, Mukkafa S, Hurana AI, Ankidawa BA. 2019. Delineation of aquifer potential zones using hydraulic parameters in Gombe and environs, North-Eastern, Nigeria. Heliyon, 5 e01927. Doi: 10.1016/j.heliyon.2019.e01927

Loureiro GE and Lisboa EG. 2011. Comparação dos métodos de interpolação especial aplicados a dados pluviométricos da região hidrográfica Tocantins-Araguaia. In: XIX Simpósio Brasileiro de Recursos Hídricos, Maceió, AL, Brazil. Proceedings. Doi: 10.13140/RG.2.1.1112.2721

Lucena LRF. 2005. Implicação da compartimentação estrutural no Aquífero Barreiras na área da bacia do Rio Pirangi-RN. PhD Thesis. Universidade Federal do Paraná – UFPR, Curitiba, Brazil. 151 pp.

Lucena LRF, Dantas JA, Medeiros AA, Rosa Filho EF. 2013a. A lixiviação de fertilizantes nitrogenados na zona não saturada superior do Aquífero Barreiras – área da bacia do Rio Catu – RN. Revista Águas Subterrâneas, 27(1): 79-91. Doi: 10.14295/ras.v27i1.27338

Lucena LRF, Oliveira Jr JG, Medeiros, WE, Queiroz, MA. 2013b. The potential of the Barreiras Aquifer in the lower course of the Doce River, Rio Grande do Norte, northeast Brazil – Integration of hydrogeological and geophysical data. Brazilian Journal Geophysics, 31(1): 43-57.

Martinez-Bastida JJ, Arauzo M, Valladolid M. 2010. Intrinsic and specific vulnerability of groundwater in central Spain: the risk of nitrate pollution. Hydrogeology Journal, 18: 681-698.

Doi: 10.1007/s10040-009-0549-5

Mendoza JA and Barmen G. 2006. Assessment of groundwater vulnerability in the Río Artiguas Basin, Nicaragua. Environmental Geology, 50: 569-580. Doi: 10.1007/s00254-006-0233-1

Nunes LMG, Lucena LRF, Silva CCN. 2019. Reserve evaluation of a fault-conditioned aquifer: the Barreiras Aquifer in the coastal region of NE Brazil. Brazilian Journal of Geology, 49(4): e20180127. Doi: 10.1590/2317-4889202020180127

Oni TE, Omosuyi GO, Akinlalu AA. 2017. Groundwater vulnerability assessment using hydrogeologic and geoelectric layer susceptibility indexing at Igbara Oke, Southwestern Nigeria. NRIAG Journal of Astronomy and Geophysics, 6(2017): 452-458. Doi: 10.1016/j.nrjag.2017.04.009

Orellana E.1972. Prospeccion geoelectrica en corriente continua. Ed. Paraninfo. Madrid. 523 pp.

Reynolds JM. 2011. An introduction to applied and environmental geophysics. UK: Ed. Wiley-Blackwell, 2nd ed., 712 pp.

Rossetti DF, Bezerra FHR, Góes AM, Valeriano MM, Andrades-Filho CO, Mittani JCR, Tatumi SH, Brito-Neves BB. 2011. Late Quaternary sedimentation in the Paraíba Basin, Northeastern Brazil: Landform, sea level and tectonics in Eastern South America passive margin. Palaeogeography, Palaeoclimatology, Palaeoecology, 300: 191-204. Doi: 10.1016/j.palaeo.2010.12.026

Silva LRD, Lucena LRF, Vieira MM, Nascimento AF. 2014. Estimativa de parâmetros hidráulicos do Aquífero Barreiras-RN a partir de análise computacional de imagens de lâminas delgadas. Revista Águas Subterrâneas, 28(2): 14-27. Doi: 10.14295/ras.v28i2.27873

Souza IVF, Lucena LRF, Bezerra FHR, Diniz Filho JB. 2019. Use of hydrogeophysical data to determine the role of faults in the geometry of the Barreiras Aquifer, Brazil. Brazilian Journal of Geology, 49(2): e20170141. Doi: 10.1590/2317-4889201920170141

Stein P, Cabral MNT, Manoel Filho J, Lucena LRF. 2019. Efeito da descontinuidade estrutural na hidrogeoquímica do aquífero Barreiras no nordeste do Brasil. Revista Águas Subterrâneas, 33(1): 45-57. Doi: 10.14295/ras.v33i1.29225

SURFER. 2002. Contouring and 3D Surface Mapping for Scientists and Engineers. Golden Software, Inc. Golden, Colorado, USA.

Yusuf SN, Ishaku JM, Wakili WM. 2021. Estimation of Dar-Zarrouk parameters and delineation of groundwater potential zones in Karlahi, part of Adamawa Massif, Northeastern Nigeria. Warta Geologi, 47(2): 103-112. Doi: 10.7186/wg472202101

A.R.O.M.: writing of the first manuscript draft and preparing of all figures; **L.R.F.L.:** advisorship regarding the methodology and its applications, and manuscript improvement with corrections and suggestions.

Received on August 31, 2021 / Accepted on March 23, 2022